J. Fluid Mech. (2020), *vol*. 904, R2, doi:10.1017/jfm.2020.765

JFM RAPIDS
journals.cambridge.org/rapids

Self-similarity in the breakup of very dilute viscoelastic solutions

A. Deblais[1],†, M. A. Herrada[2], J. Eggers[3] and D. Bonn[1]

[1]Van der Waals–Zeeman Institute, Institute of Physics, University of Amsterdam, 1098XH Amsterdam, The Netherlands

[2]Departamento de Mecánica de Fluidos e Ingeniería Aeroespacial, Universidad de Sevilla, 41092 Sevilla, Spain

[3]School of Mathematics, University of Bristol, Fry Building, Woodland Road, Bristol BS8 1UG, UK

(Received 3 May 2020; revised 8 September 2020; accepted 9 September 2020)

When pushed out of a syringe, polymer solutions form droplets attached by long and slender cylindrical filaments whose diameter decreases exponentially with time before eventually breaking. In the last stages of this process, a striking feature is the self-similarity of the interface shape near the end of the filament. This means that shapes at different times, if properly rescaled, collapse onto a single universal shape. A theoretical description based on the Oldroyd-B model was recently shown to disagree with existing experimental results. By revisiting these measurements and analysing the interface profiles of very diluted polyethylene oxide solutions at high temporal and spatial resolution, we show that they are very well described by the model.

Key words: liquid bridges, viscoelasticity

1. Introduction

The formation of drops has become a paradigm for the study of singularities in fluid mechanics and beyond. The formation of a drop from an orifice leads to a new length scale, the diameter of the neck that connects the drop to the orifice, which goes to zero at a finite time when the drop breaks off from the orifice. As a result, pinch-off is described by a similarity solution that describes the time evolution and self-similar shape of the neck close to breakup. In the case of Newtonian fluids of both large and small viscosity, the neck diameter behaves like a power law as a function of the time to pinch-off. The interface is found to have a universal shape, and profiles at different times can be superimposed onto one another by rescaling the radial and axial coordinates by appropriate powers of the time distance to the singularity.

† Email address for correspondence: a.deblais@uva.nl

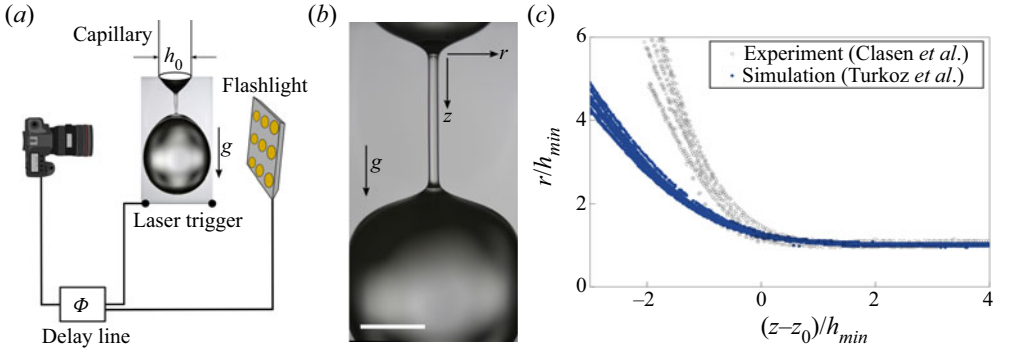

FIGURE 1. (*a*) Schematic of the experimental set-up used to determine the interface shape of the polymer thread. A full-frame camera is combined with a flashlight allowing short flash duration. The flash is triggered on the falling drop and a high-accuracy delay line allows one to follow the breakup event in time by taking pictures at different delays. (*b*) Typical photograph of a pendent drop of a very dilute polymer solution breaking from a syringe. A long tiny polymer thread connecting the two drops is formed. Scale bar is 1 mm. (*c*) Self-similar thinning of the interface profiles obtained from the experimental work of Clasen *et al.* (2006) and the simulations of Turkoz *et al.* (2018). Here z_0 is the axial location for which the profiles collapse best. The comparison reveals a discrepancy between the two. Figure adapted from Turkoz *et al.* (2018).

Beyond Newtonian fluids, much work has been dedicated to the formation of drops in non-Newtonian fluids such as polymer solutions. These fluids are characterized by a slow time scale λ on which the constituents relax. If one takes a dilute solution of a high-molecular-weight polymer and tries to make a droplet (Middleman 1965; Goldin *et al.* 1969; Petrie & Denn 1976; Eggers 1997; Deblais, Velikov & Bonn 2018), polymers become stretched in the extensional flow close to pinch-off, and long and slender filaments form in between drops, where previously power-law pinch-off would have been observed (Goldin *et al.* 1969; Bazilevskii *et al.* 1981; Entov & Yarin 1984; Wagner *et al.* 2004; Clasen *et al.* 2006; Bhat *et al.* 2010). In the case of a jet, this means a long sequence of almost circular drops form, connected by tiny threads, a phenomenon that has been called the 'beads-on-a-string' structure. In the case of a dripping tap (faucet), one observes essentially the same phenomenon, except that here only a single drop forms, with perhaps a satellite drop in between (Wagner *et al.* 2004), connected to the tap (faucet) by a tiny thread, as seen in figure 1(*a*,*b*).

This and similar phenomena are often modelled using the so-called Oldroyd-B model (Bird, Armstrong & Hassager 1987), which describes the polymer relaxation with a single time scale λ. The stress is written as the sum of a polymeric contribution and that of the solvent.

The formation of filaments and their instabilities have by now become a benchmark problem for testing viscoelastic fluid mechanics (Anna & McKinley 2001; McKinley & Sridhar 2002; Furbank & Morris 2004; Suryo & Basaran 2006; Smith *et al.* 2010; Huisman, Friedman & Taborek 2012; Miskin & Jaeger 2012). Instead of following a power law, the filament now thins exponentially with a rate set by the relaxation time of the polymer (Bazilevskii *et al.* 1981; Anna & McKinley 2001; Clasen *et al.* 2006). The profile is extremely uniform over the thread, and then merges smoothly with a neighbouring drop on either side. It was proposed by Clasen *et al.* (2006) that the profile at this junction is once more a similarity solution, which yields a universal profile, if both the axial and the radial coordinates are rescaled with the thread radius, with an exponential rise

towards the drop (figure 1*c*). Clasen *et al.* (2006) were able to calculate the similarity profile using a lubrication approximation, in which the interface slope is assumed small; however, this assumption of small slopes is not satisfied throughout the profile. Indeed, while an experiment using long flexible polymers in a viscous solvent showed collapse to a self-similar profile, a comparison with the theoretical calculation revealed an axial length scale in the experiment that was about twice as short as the one obtained from lubrication theory (figure 1*c*). At the time, this serious discrepancy in the self-similar profile was attributed to a failure of the lubrication approximation.

However, a recent full numerical simulation of the Oldroyd-B equations (Turkoz *et al.* 2018) showed the same discrepancy with the experimental data of Clasen *et al.* (2006), and rather agreed with the lubrication calculation (figure 1*c*). This left the serious possibility that the source of the discrepancy was the Oldroyd-B model itself. One possibility was that the experimental fluid was described by more than a single length scale, the other that the finite extensibility of a real polymer has to be taken into account, as described, for example, by more elaborate models such as the FENE-P model (Bird *et al.* 1987), which also describes the shear-thinning behaviour of a real polymeric fluid.

More recently, the similarity theory of Clasen *et al.* (2006) was extended to a treatment of the full axisymmetric Oldroyd-B equations, and the similarity profile was calculated without any lubrication assumptions (Snoeijer *et al.* 2019). The robustness of these calculations was also underlined by the observation that the universal interface shape even holds for purely elastic filaments undergoing elasto-capillary instabilities (Snoeijer *et al.* 2019; Eggers, Herrada & Snoeijer 2020) that could be dubbed sausage-on-a-string instabilities (Mora *et al.* 2010; Kibbelaar *et al.* 2020). These findings suggest that the specific type of viscoelastic model for the polymer solution is not crucial for calculating the shape of the interface, and hence could not explain the discrepancy between theory and experiment.

To clear up these questions, we investigate the breakup of very dilute polymer solutions. We record the interface profiles of the filaments at an extremely high temporal and spatial resolution during the experiments, and compare the results with the newly developed similarity theory of Eggers *et al.* (2020), based on the full Oldroyd-B equations. Our results convincingly show that the experimental profiles all converge to a universal self-similar solution that in addition agrees excellently with theory.

2. Experiments

We experimentally study the extensional thinning and destabilization of filaments of long-chain polymer solutions in water at different concentrations (figure 2). The experiments are performed with polyethylene oxide (PEO) with a molecular weight (M_w) of $(4 \pm 2) \times 10^6$ g mol^{-1} (Berman 1978) from Sigma-Aldrich (purity = 0.98). Four concentrations C_p between 10 and 120 w.p.p.m. (weight parts per million) are obtained from successive dilutions of the initial batch. This range of concentrations is chosen to be well below the critical overlap concentration of polymer coils (Graessley 1980):

$$c^* = \frac{0.77}{[\eta]}, \tag{2.1}$$

with $[\eta]$ the intrinsic viscosity of the polymer solution (see details in table 1, from Del Giudice, Haward & Shen (2017)). The concentrations we consider allow us to work in conditions that are very close to satisfying the Oldroyd-B model, as we will show below.

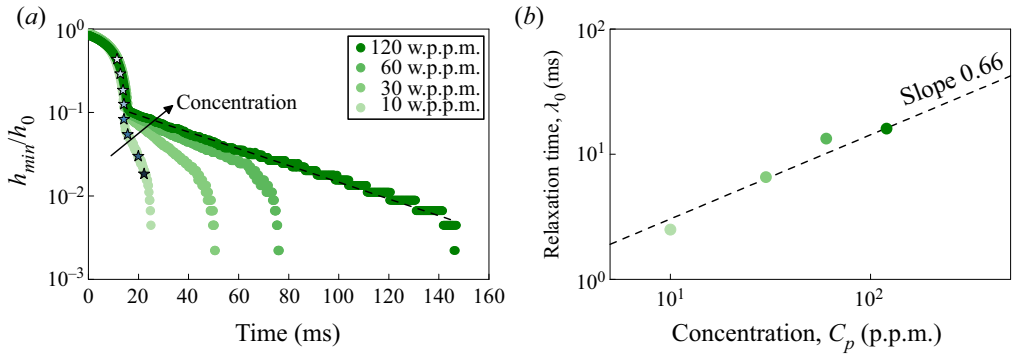

FIGURE 2. Thinning dynamics of a filament of four concentrations of polyethylene oxide in water. (*a*) Symbol colours, from light to dark: 10, 30, 60 and 120 w.p.p.m. (weight parts per million). The minimum neck radius h_{min} is tracked in time and normalized by the inner radius h_0 of the syringe orifice; the longest relaxation time of the solution λ_0 is deduced from the slope of the elasto-capillary regime highlighted by the dashed black line. (*b*) Relaxation time λ_0 as a function of the concentration C_p. The dashed line is a power-law fit to the experimental points $\lambda_0 \propto C_p^{0.66}$.

A syringe pump supplies the polymer solutions to the needle tip (inner diameter $h_0 = 2$ mm).

We used a Phantom V1 fast camera (frame rate 10 000 frames per second) to record the dynamics of the filament thinning at a high temporal resolution, and a full-frame camera (8256 pixel $\times$ 4640 pixel, Nikon D850) equipped with a 5$\times$ microscope lens to obtain a very good spatial resolution of the polymer interface during its detachment. In order to be able to capture high-quality pictures of the interface during the fast thinning ($\sim$ milliseconds), we use a flashlight (Vela one) with 1 μs flash duration. The camera and the flashlight are coupled to a trigger to which we can control the delay to the next breakup event with a very good accuracy. The delay between two flashes is controlled through a precise delay line (Digital Delay Generator, DG535 Stanford Research Systems) that delays the initial trigger pulse (the event is triggered electronically on each bottom edge of droplets falling in repetition) and allows a delay resolution from 5 ps to 1000 s. The limiting factor here is the flash duration of 1 μs of the flashlight itself. The shutter of the camera is open for a 'long' time during the flash, and so the read-out time of the camera is not a limiting step. This allow us to obtain a sequence of very highly resolved pictures (10 μm pixel^{-1}) as one would obtain with a fast camera but with a much better resolution (see sequence of pictures in figure 3).

Typical results are shown in figures 2 and 3. The thinning dynamics (figure 2) of PEO show an initial thinning similar to that of a low-viscosity Newtonian fluid. Subsequently, a very long and slender cylindrical filament is formed. In this elasto-capillary thinning regime, the dynamics slows down dramatically. Both the Oldroyd-B model and experiments show that in this regime the minimum neck radius h_{min} as a function of time can be described as

$$h_{min} = h_0\, \mathrm{e}^{-t/3\lambda_0}, \tag{2.2}$$

with λ_0 the longest relaxation time of the polymer solution (Amarouchene *et al.* 2001; Anna & McKinley 2001). In the range of (very) diluted concentrations studied here,

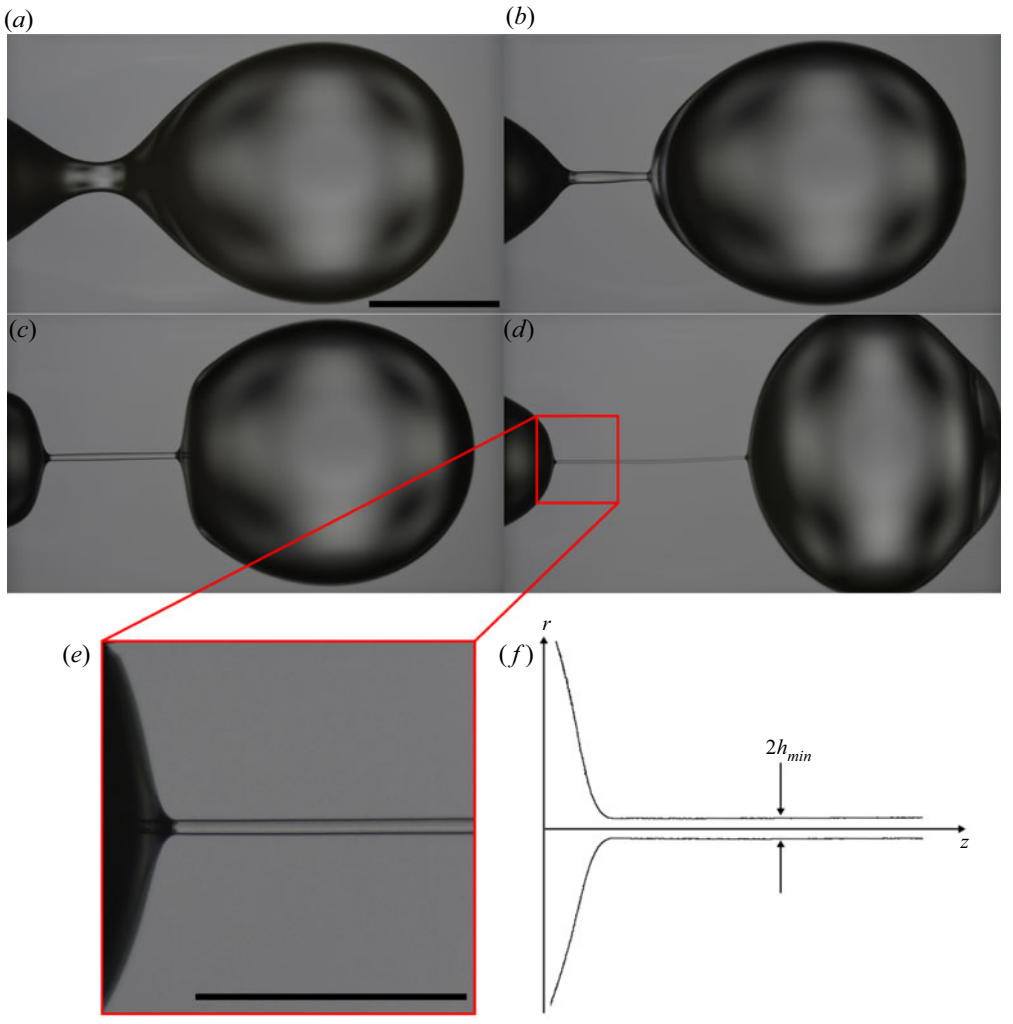

FIGURE 3. High-resolution photographs of a pendent drop of PEO solution ($M_w = 4 \times 10^6$ g mol^{-1}, $C_p = 10$ w.p.p.m.) breaking from a nozzle of diameter $h_0 = 2$ mm. The time between subsequent panels (*a–d*) is 1 ms. Scale bar is 2 mm. Panel (*e*) highlights the region of interest from which we extract the profile shown in panel (*f*). Scale bar is 1 mm.

λ_0 varies with concentration between $\sim$1 and 50 ms. Even though in the dilute limit a variation of the relaxation time is not predicted by theory, this is in fact commonly observed in experiments (Clasen *et al.* 2006). This is confirmed by plotting the dependence of the relaxation time λ_0 with the polymer concentration C_p in figure 2(*b*), showing that it follows a power-law dependence as reported by Clasen *et al.* (2006) for dilute polymer solutions.

Figure 3 shows a typical sequence of pictures of a droplet's interface, obtained using the combination of fast camera and triggered flash to increase the resolution. We use these photographs to extract the interface profile with a homemade algorithm in MATLAB; this procedure allows determination of the edges of the polymer solution as shown in figure 3(*f*).

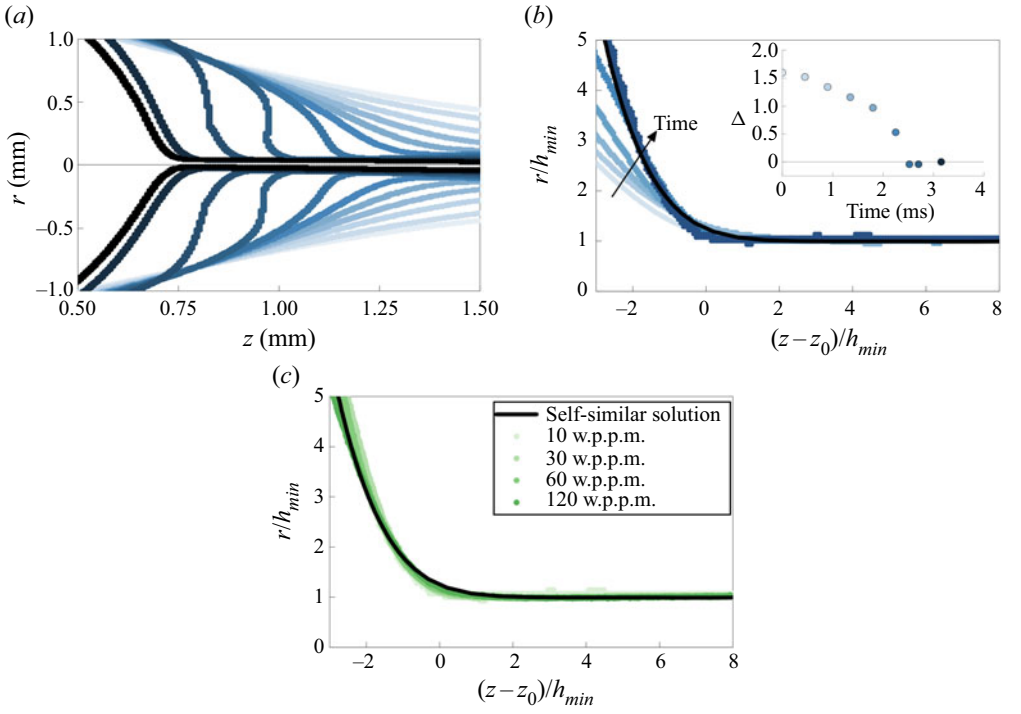

FIGURE 4. (*a*) Time evolution of PEO filament profiles near the onset of the filament. Data are shown for subsequent times between each profile that are highlighted in figure 2(*a*) (star symbols) and for $C_p = 10$ w.p.p.m. (*b*) Same profiles but rescaled by the minimum neck radius h_{min} and with z_0 the location for which the experimental profiles beyond a time threshold collapse onto each other. The inset shows the convergence of the quantity $\Delta(t)$ towards the self-similar solution. (*c*) Post-threshold profiles for four polymer concentrations in the dilute regime. In panels (*b*) and (*c*), the solid black line indicates a universal self-similar solution calculated using the Oldroyd-B model.

C_p (w.p.p.m.)	$[\eta]$ (m^3 kg^{-1})	c^*	C_p/c^*	n (10^{18} m^{-3})
10	1.408	0.071	0.014	1.51
30	1.408	0.071	0.042	4.52
60	1.408	0.071	0.084	9.03
120	1.408	0.071	0.169	18.1

TABLE 1. Physical parameters of the polymer solutions investigated (PEO) with a molecular weight of $M_w = 4 \times 10^6$ g mol^{-1}.

3. Results

In figure 4(*a*) we show the evolution of the interface profile during filament thinning, near the drop that forms due to destabilization. Here, r is the filament radius and z the direction along the filament. In figure 4(*b*), we plot the same profiles but rescaled by the minimum neck radius h_{min} and with z_0 an adjustable parameter that represents the location for which the experimental profiles collapse best. As time progresses, the interface shape

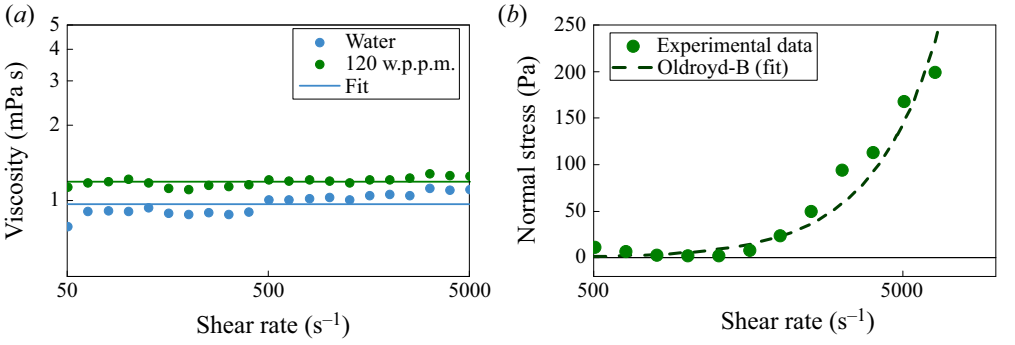

FIGURE 5. (*a*) Shear rheology of a PEO solution (green symbols; $M_w = 4 \times 10^6$ g mol^{-1}, $C_p = 120$ w.p.p.m.) compared to water (blue symbols) for shear-rate values allowed by our experimental set-up. (*b*) Magnitude of the first normal stress difference N_1 as a function of shear rate for a PEO solution ($C_p = 120$ w.p.p.m.). Dashed line is a fit of the Oldroyd-B model (3.1).

converges to a universal shape. Comparing this shape to the recent viscoelastic calculations using the Oldroyd-B model (Eggers *et al.* 2020), we find an excellent agreement: the profiles converge to the same universal self-similar solution profile indicated by the black line. We quantify the threshold to the self-similar solution by measuring the distance $\Delta(t)$ of the experimental profiles to the self-similar curve at $r/h_{min} = \exp(1)$. This quantity is shown in the inset of figure 4(*b*) and converges to a constant value at the moment where the elasto-capillary regime is reached. Since the onset is set by the elasto-capillary time, a dependence with the polymer concentration C_p is expected. In figure 4(*c*), we show the profiles after converging for different polymer concentrations. They fall onto each other, confirming the self-similarity of the polymer thread interface. Here, again, agreement with theory (black line) is excellent; this also confirms that the profile grows exponentially, as discussed in detail in Eggers *et al.* (2020).

Solving the constitutive equation for a Hookean dumbbell model, a quadratic dependence of the first normal stress difference N_1 on shear rate $\dot{\gamma}$ can be obtained (Bird *et al.* 1987):

$$N_1(\dot{\gamma}) = \psi_1 \dot{\gamma}^2 = 2nk_BT\lambda_{0,rheo}^2 \dot{\gamma}^2, \tag{3.1}$$

with T denoting temperature, ψ_1 the first normal stress coefficient, n the number density of polymer molecules (table 1) and k_B Boltzmann's constant. The rheology measurements (Anton Paar, MCR 302) shown in figure 5(*a*) show that the increase in polymer concentration slightly influences the shear viscosity, in agreement with Einstein expansion, whereas it significantly affects the normal force (figure 5*b*), from which we can extract the relaxation time of the solution $\lambda_{0,rheo} = 7.4$ ms (Lindner, Vermant & Bonn 2003). This is a factor ~ 2 below the value obtained with the relaxation time obtained from the pinch-off experiment ($\lambda_0 = 14.5$ ms). Such discrepancies have already been reported before by Clasen *et al.* (2006). The primary reason for the discrepancy is that high-molecular-weight polymers invariably exhibit a significant polydispersity, which may result in multiple time scales; the elongational flow is more sensitive to the longest time scale, whereas the shear flow probes an average time scale. We can nevertheless evaluate the ratio between these two time constants using the multimode Zimm model:

$$\langle\lambda\rangle \approx \lambda_{0,rheo} = \frac{1}{N}\sum_i \lambda_i = \frac{1}{N}\sum_i \frac{\lambda_0}{i^{2+\tilde{\sigma}}}, \tag{3.2}$$

where N is the total number of modes and $\tilde{\sigma}$ is a measure of the hydrodynamics interaction, with $\tilde{\sigma} \approx -0.4$ in our dilute polymer solutions (Anna & McKinley 2001). This time quickly decays for the higher modes; evaluating the ratio between the two time scales for the five first modes gives a good approximation. In fact, this gives a value of $\lambda_{0,rheo}/\lambda_0 \approx 3$, which is a good estimate of what we find experimentally and is a value also reported experimentally by Liang & Mackley (1994).

4. Conclusions

In conclusion, we have studied the destabilization of diluted polyethylene oxide (PEO) solution in water using a camera set-up allowing us to visualize the droplet and filament shapes with very high resolution. We find that, during destabilization of a polymer droplet initially attached to a capillary, the interface converges to a self-similar shape independent of time or polymer concentration, which agrees very well with the theoretical prediction of Eggers *et al.* (2020), based on the Oldroyd-B model. This contrasts with an earlier discrepancy, observed in Turkoz *et al.* (2018), between full numerical simulations of the Oldroyd-B model and the earlier experiments of Clasen *et al.* (2006).

Three main differences between our experiment and that of Clasen *et al.* (2006) can be mentioned that might explain the observed discrepancy. (i) In the work presented here we are now able to work at significantly higher spatial and temporal resolution than they could do at the time. (ii) The second important difference to note is the solvent used, which is much more viscous than the one we use in our study (water) and also exhibits non-Newtonian behaviour ('Boger fluid'). (iii) They used a Caber device to impose an extensional deformation to their samples. For that purpose, they used endplate diameters up to 6 mm (three times our nozzle diameter D_{min}). As a consequence, gravitational and inertial effects may have an effect on the overall extensional flow: it consequently may generate additional flows during the thinning of the filament and affect the profile of the interface, as discussed for instance in Brady & Acrivos (1982).

Acknowledgements

A.D. acknowledges funding from the EU's Horizon 2020 research and innovation programme under the Individual Marie Skłodowska-Curie fellowship grant agreement 798455. M.A.H. acknowledges the support of the Junta de Andalucia through grant P18-FR-3623.

Declaration of interests

The authors report no conflict of interest.

References

Amarouchene, Y., Bonn, D., Meunier, J. & Kellay, H. 2001 Inhibition of the finite-time singularity during droplet fission of a polymeric fluid. *Phys. Rev. Lett.* **86**, 3558–3561.

Anna, S. L. & McKinley, G. H. 2001 Elasto-capillary thinning and breakup of model elastic liquids. *J. Rheol.* **45** (1), 115–138.

Bazilevskii, A. V., Voronkov, S. I., Entov, V. M. & Rozhkov, A. N. 1981 Orientational effects in the decomposition of streams and strands of diluted polymer solutions. *Sov. Phys. Dokl.* **26**, 333–335.

BERMAN, N. S. 1978 Drag reduction by polymers. *Annu. Rev. Fluid Mech.* **10** (1), 47–64.

BHAT, P. P., APPATHURAI, S., HARRIS, M. T., PASQUALI, M., MCKINLEY, G. H. & BASARAN, O. A. 2010 Formation of beads-on-a-string structures during break-up of viscoelastic filaments. *Nat. Phys.* **6** (8), 625–631.

BIRD, R. B., ARMSTRONG, R. C. & HASSAGER, O. 1987 *Dynamics of Polymeric Liquids. Vol. 1: Fluid Mechanics*. John Wiley and Sons.

BRADY, J. F. & ACRIVOS, A. 1982 The deformation and breakup of a slender drop in an extensional flow: inertial effects. *J. Fluid Mech.* **115**, 443–451.

CLASEN, C., EGGERS, J., FONTELOS, M. A., LI, J. & MCKINLEY, G. H. 2006 The beads-on-string structure of viscoelastic threads. *J. Fluid Mech.* **556**, 283–308.

DEBLAIS, A., VELIKOV, K. P. & BONN, D. 2018 Pearling instabilities of a viscoelastic thread. *Phys. Rev. Lett.* **120** (19), 194501.

DEL GIUDICE, F., HAWARD, S. J. & SHEN, A. Q. 2017 Relaxation time of dilute polymer solutions: a microfluidic approach. *J. Rheol.* **61** (2), 327–337.

EGGERS, J. 1997 Nonlinear dynamics and breakup of free-surface flows. *Rev. Mod. Phys.* **69** (3), 865–930.

EGGERS, J., HERRADA, M. A. & SNOEIJER, J. H. 2020 Self-similar breakup of polymeric threads as described by the Oldroyd-B model. *J. Fluid. Mech.* **887**, A19.

ENTOV, V. M. & YARIN, A. L. 1984 Influence of elastic stresses on the capillary breakup of jets of dilute polymer solutions. *Fluid Dyn.* **19** (1), 21–29.

FURBANK, R. J. & MORRIS, J. F. 2004 An experimental study of particle effects on drop formation. *Phys. Fluids* **16** (5), 1777–1790.

GOLDIN, M., YERUSHALMI, J., PFEFFER, R. & SHINNAR, R. 1969 Breakup of a laminar capillary jet of a viscoelastic fluid. *J. Fluid Mech.* **38** (4), 689–711.

GRAESSLEY, W. W. 1980 Polymer chain dimensions and the dependence of viscoelastic properties on concentration, molecular weight and solvent power. *Polymer* **21** (3), 258–262.

HUISMAN, F. M., FRIEDMAN, S. R. & TABOREK, P. 2012 Pinch-off dynamics in foams, emulsions and suspensions. *Soft Matt.* **8** (25), 6767–6774.

KIBBELAAR, H. V. M., DEBLAIS, A., BURLA, F., KOENDERINK, G. H., VELIKOV, K. P. & BONN, D. 2020 Capillary thinning of elastic and viscoelastic threads: from elastocapillarity to phase separation. *Phys. Rev. Fluids* **5** (9), 092001.

LIANG, R. F. & MACKLEY, M. R. 1994 Rheological characterization of the time and strain dependence for polyisobutylene solutions. *J. Non-Newtonian Fluid Mech.* **52** (3), 387–405.

LINDNER, A., VERMANT, J. & BONN, D. 2003 How to obtain the elongational viscosity of dilute polymer solutions? *Physica* A **319**, 125–133.

MCKINLEY, G. H. & SRIDHAR, T. 2002 Filament-stretching rheometry of complex fluids. *Annu. Rev. Fluid Mech.* **34** (1), 375–415.

MIDDLEMAN, S. 1965 Stability of a viscoelastic jet. *Chem. Engng Sci.* **20** (12), 1037–1040.

MISKIN, M. Z. & JAEGER, H. M. 2012 Droplet formation and scaling in dense suspensions. *Proc. Natl Acad. Sci. USA* **109** (12), 4389–4394.

MORA, S., PHOU, T., FROMENTAL, J. M., PISMEN, L. M. & POMEAU, Y. 2010 Capillarity driven instability of a soft solid. *Phys. Rev. Lett.* **105** (21), 214301.

PETRIE, C. J. S. & DENN, M. M. 1976 Instabilities in polymer processing. *AIChE J.* **22** (2), 209–236.

SMITH, M. I., BESSELING, R., CATES, M. E. & BERTOLA, V. 2010 Dilatancy in the flow and fracture of stretched colloidal suspensions. *Nat. Commun.* **1** (1), 1–5.

SNOEIJER, J. H., PANDEY, A., HERRADA, M. A. & EGGERS, J. 2019 The relationship between viscoelasticity and elasticity. arXiv:1905.12339.

SURYO, R. & BASARAN, O. A. 2006 Local dynamics during pinch-off of liquid threads of power law fluids: scaling analysis and self-similarity. *J. Non-Newtonian Fluid Mech.* **138** (2–3), 134–160.

TURKOZ, E., LOPEZ-HERRERA, J. M., EGGERS, J., ARNOLD, C. B. & DEIKE, L. 2018 Axisymmetric simulation of viscoelastic filament thinning with the Oldroyd-B model. *J. Fluid. Mech.* **851**, R2.

WAGNER, C., AMAROUCHENE, Y., BONN, D. & EGGERS, J. 2004 Droplet detachment and bead formation in visco-elastic fluids. *Phys. Rev. Lett.* **95** (16), 7–10.